

NJC

Accepted Manuscript



This is an *Accepted Manuscript*, which has been through the Royal Society of Chemistry peer review process and has been accepted for publication.

Accepted Manuscripts are published online shortly after acceptance, before technical editing, formatting and proof reading. Using this free service, authors can make their results available to the community, in citable form, before we publish the edited article. We will replace this *Accepted Manuscript* with the edited and formatted *Advance Article* as soon as it is available.

You can find more information about *Accepted Manuscripts* in the [Information for Authors](#).

Please note that technical editing may introduce minor changes to the text and/or graphics, which may alter content. The journal's standard [Terms & Conditions](#) and the [Ethical guidelines](#) still apply. In no event shall the Royal Society of Chemistry be held responsible for any errors or omissions in this *Accepted Manuscript* or any consequences arising from the use of any information it contains.

Synthesis, characterization and evaluation of diglycidyl-1,2-cyclohexanedicarboxylate crosslinked polyethylenimine nanoparticles as efficient carrier of DNA

Ruby Bansal, Pallavi Kiran and Pradeep Kumar*

Nucleic Acids Research Laboratory, CSIR-Institute of Genomics and Integrative Biology, Delhi University Campus, Mall Road, Delhi – 110 007, India

Corresponding author's address

Dr. Pradeep Kumar

Nucleic Acids Research Laboratory,

CSIR-Institute of Genomics and Integrative Biology,

Delhi University Campus, Mall Road, Delhi – 110 007, India

Email: pkumar@igib.res.in; pkumar@igib.in

Tel.: +91 11 27662491; Fax: +91 11 27667471

Non-viral gene delivery vectors have shown promising potential to treat a variety of inherited and acquired disorders. Among various non-viral systems, cationic polymers have proved to be the most efficient gene carriers as they have tendency to condense nucleic acids to nanosized particles and improve their transfer inside the cells. Polyethylenimine has been considered as ‘gold standard’ in gene delivery applications. However, charge-associated toxicity has limited its clinical efficacy. Here, we have tried to address this concern by partially reducing the cationic charge density on branched polyethylenimine (PEI, 10 and 25 kDa) and simultaneously converting these polymers into their respective nanoparticles using a commercially available reactive crosslinking reagent, diglycidyl-1,2-cyclohexanedicarboxylate (DCD). Varying the amounts of DCD during crosslinking reaction generated two small series of diglycidyl-1,2-cyclohexanedicarboxylate-PEI (DP₁₀ and DP₂₅) nanoparticles with size ranged from 125-201 nm and zeta potential from +11-20 mV. Though these nanoparticles showed no difference in the nucleic acid condensing ability from their respective native polymers, the buffering capacity showed a significant decrease as determined by acid-base titration method. On further evaluation, pDNA complexes of the DP₁₀ and DP₂₅ nanoparticles were found to be non-toxic and exhibited several folds higher transfection efficiency than native polymers and the standard transfection reagent, Lipofectamine. Altogether, these results demonstrate that these nanoparticles can effectively be used for future gene delivery applications.

Keywords: Polyethylenimine; nanoparticles; cytotoxicity; transfection; plasmid DNA

1. Introduction

Synthetic cationic polymers have recently shown their potential in delivering exogenous nucleic acids in safe and efficient manner inside the cells.¹⁻⁴ Ease of their synthesis and amenability to modifications have attracted the attention of the researchers working in the area of gene therapy. Among the various synthetic cationic polymers, polyethylenimine (PEI) has been the most extensively used.⁵⁻⁸ High cationic charge and the presence of a variety of amines (primary, secondary and tertiary) have made it a versatile polymer that has capability to condense nucleic acids, provide protection against nucleases and promote their uptake. Molecular weight, structure and molecular composition of a polymer play an important role in these processes.⁹ Basically, PEIs are available in two forms, i.e. branched and linear. Efficiency of these polymers to transport nucleic acids depends upon their molecular weight, which varies from 0.4 to 750 kDa. High molecular weight PEIs exhibit high transfection efficiency but are toxic while low molecular weight PEIs are non-toxic but display poor transfection efficiency.¹⁰ Moreover, of the two forms, branched PEIs show higher efficiency as compared to linear ones. Therefore, bPEI (25 kDa) is considered as a 'gold standard' in gene delivery applications¹¹⁻¹³ but displays charge-associated cytotoxicity, which hampers its clinical efficacy. To overcome this drawback, several modifications have been incorporated and modified analogs have been synthesized that have been shown to possess better transfection efficiency with lower cytotoxicity.¹³⁻¹⁶ The successful design of a gene delivery vector requires a subtle balance between transfection efficiency and cytotoxicity. Cytotoxicity of bPEIs has been addressed in two ways without compromising on the transfection efficiency. In one of the ways, hydrophobic ligands have been introduced in the polymeric chains, which have lowered the cytotoxicity due to reduction in the overall cationic charge density.¹⁷⁻¹⁹ As a result, transfection efficiency also increased because of improved interactions with the lipidic constituents of the cell membranes. However, higher degree of substitution of such ligands has affected the solubility of the polymers in cell culture medium. In another way, hydrophilic homobifunctional crosslinkers have been employed that have capability to convert PEIs into their respective nanoparticles.^{20,21} These crosslinkers react with primary or secondary or both types of amines and decrease the overall cationic charge density due to conversion of primary to secondary and secondary to tertiary amines. The resulting nanoparticles have shown reduced cytotoxicity and display certain advantages such as (i) easy uptake and internalization in the cells, (ii) being compact in size (in the range of nanometers), they are less susceptible to reticuloendothelial system (RES) clearance and (iii) these

particles exhibit greater penetration into the cells and tissues.^{22,23} Encouraged by these findings, we hypothesized that crosslinking using a lipophilic homobifunctional reagent would not only form the nanoparticles of the bPEIs but also improve their uptake and internalization via hydrophobic interactions. Therefore, in the present study, we have selected a lipophilic homobifunctional reagent, diglycidyl-1,2-cyclohexanedicarboxylate, crosslinked two variants of bPEI (10 and 25 kDa) and investigated the effect of molecular weight on the transfection efficiency. By varying the amounts of the crosslinker, two series of DP nanoparticles were synthesized and evaluated for their cytotoxicity and transfection efficiency. These nanoparticle/pDNA complexes exhibited higher transfection efficiency than their corresponding bPEI/pDNA complexes as well as the standard transfection reagent, Lipofectamine 2000. Cytotoxicity of the complexes showed a marked decrease compared to their native complexes. It also showed a decrease with an increase in the degree of substitution of the crosslinker.

2. Materials and methods

2.1. Materials

Branched polyethylenimine (bPEI, 25 kDa), 3-(4,5-dimethylthiazol-2-yl)-2,5-diphenyltetrazolium bromide (MTT), ethidium bromide (EtBr), orange G dye, Dulbecco's Modified Eagle Medium (DMEM) and dialysis membrane (MWCO 12 kDa) were procured from Sigma-Aldrich Chemical Company (USA). Branched polyethylenimine (bPEI, 10 kDa) was purchased from Polysciences Inc., USA. Lipofectamine 2000 was obtained from Invitrogen (USA). Other reagents and chemicals, used in the present study, were purchased from local vendors. Particle size (hydrodynamic diameter) and zeta potential measurements were performed on Zetasizer Nano-ZS (Malvern Instruments, UK). Size and morphology of the particles were also determined by high-resolution transmission electron microscopy (HR-TEM, Tecnai G2 30U-twin 200kV electron microscope). Enhanced green fluorescent protein plasmid (pEGFPN3, 4.4 Kbp) was used in the transfection and cytotoxicity assays and its expression was observed under Nikon Eclipse TE 2000-S inverted microscope (Kanagawa, Japan). Quantitative estimation of green fluorescent protein (GFP) was carried out on NanoDrop® ND-3300 spectrofluorometer, USA, at an excitation wavelength of 488 nm and emission at 509 nm. MCF-7 cells (Breast cancer cell line) were obtained from National Centre for Cell Science (NCCS), Pune, India and grown in DMEM as per the recommendations.

2.2. Synthesis of diglycidyl-1,2-cyclohexanedicarboxylate crosslinked bPEI nanoparticles (DP NPs)

Branched PEI (86 mg, 2 mmol, 10 kDa) was dissolved in Milli Q water (86 ml, 1 mg/ml). Diglycidyl-1,2-cyclohexanedicarboxylate (5.7 mg for 2% crosslinking) was taken up in tetrahydrofuran (5 ml) and added dropwise to the stirred solution of the above solution over a period of 5 min. The reaction was further stirred at an ambient temperature for 48h. Then, the reaction mixture was concentrated in vacuo to one tenth of the total volume and poured in a dialysis bag. The dialysis was proceeded for 24 h with intermittent change of water after 6h of interval. The solution was lyophilized in a speed vac to obtain DP₁₀-1 nanoparticles as white powder. Similarly, other preparations (DP10-2, DP10-3 and DP10-4 with 4, 6 and 8% crosslinking) were synthesized and lyophilized. Similarly, synthesis of DP₂₅-1, DP₂₅-2, DP₂₅-3 and DP₂₅-4 nanoparticles with 2, 4, 6 and 8% crosslinking was carried out except using bPEI (25 kDa) instead of bPEI (10 kDa). The lyophilized nanoparticles were obtained in white powdery form. Both the series of nanoparticles were characterized by ¹H-NMR.

2.3. Estimation of degree of substitution of the crosslinker in the nanoparticles

Percent substitution of the crosslinker in the nanoparticles was quantitatively estimated following a reported method with slight modification using 1-fluoro-2,4-dinitrobenzene (FDNB) reagent.²⁴ Briefly, accurately weighed amounts of DP nanoparticles (~2-3 mg) were suspended in ethanol (0.5 ml) in different vials and 0.1M solution of FDNB (0.5 ml) was added to each of the vial. The vials were then kept inside an incubator-shaker at 50°C for 1h, cooled and measured the absorbance of the reaction mixture at 356 nm. From pre-drawn standard curves using standard concentrations of PEI (10 and 25 kDa) and FDNB solution, percent substitution of the crosslinker was determined.

2.4. Preparation of pDNA complexes of DP nanoparticles

To form DNA complexes for transfection and cytotoxicity assays, appropriate amounts of aqueous solutions of DP₁₀ and DP₂₅ nanoparticles (1mg/ml) were mixed separately with a fixed amount of pDNA (1 µl of 0.3 µg / µl) to obtain various w/w ratios (0.66, 1.66, 2.33, 3.33, 4, 5, 6.66, and 10). Subsequently, 5 µl of 20% dextrose was added to the above solution before making up the final volume upto 20µl with Milli Q water. The resulting samples were gently vortexed and incubated for 30 min at RT prior to their use in biophysical studies or transfection experiments.

2.5. Physico-chemical characterization of DP nanoparticles and their pDNA complexes

Characterization of synthesized series of DP₁₀ and DP₂₅ nanoparticles was carried out by size and surface charge measurements using Dynamic Light Scattering (DLS). Plasmid DNA complexes of both the series of nanoparticles were prepared by mixing appropriate amount of the solution of nanoparticles (in water) to obtain w/w ratio at which these complexes exhibited the highest transfection efficiency. After volume was made up with water, the complexes were incubated for 30min at RT and subjected to their hydrodynamic diameter and zeta potential measurements using Zetasizer Nano-ZS. The zeta potential measurements of nanoparticles and DNA complexes were performed by carrying out 30 runs in triplicates and the average values are estimated by Smoluchowski approximation from the electrophoretic mobility and expressed in mV.

2.6. Transmission electron microscopical (TEM) analysis of pDNA complexes of DP nanoparticles

High resolution transmission electron microscopy (HR-TEM) of DP₁₀-2/pDNA and DP₂₅-4/pDNA complex was carried out on a Technai G2 30U-twin, Technai 200 kV ultra twin microscope, operating at 200 kV. The complex prepared in deionized water was deposited on carbon coated grids with 1% uranyl acetate negative staining and after drying, the image was captured at an accelerating voltage of 200 kV.

2.7. Electrophoretic mobility shift assay (EMSA) of DP/pDNA complexes

To estimate the amount of DP₁₀ and DP₂₅ nanoparticles required to completely retard the mobility of known amount of pDNA, an agarose gel electrophoresis experiment was carried out. Complexes were formed at various w/w ratios of 0.16, 0.33, 0.5, 0.60, 0.83 (DP₁₀/pDNA), 0.16, 0.33, 0.43, 0.50, 0.60, 0.83 (DP₂₅/pDNA) and 0.16, 0.23, 0.33, 0.50 (bPEI_{10,25}/pDNA) with fixed amount of 1µl DNA (300ng/µl) and incubated for 30 min at room temperature. The complexes, thus formed, were mixed with 2µl Orange G dye, electrophoresed (100V, 1h) in 0.8% agarose gel containing EtBr (2µl/100 ml gel) in 1x TAE buffer and visualized the bands in Gel Doc System (G:box UV transilluminator). A solution (20µl) containing only pDNA was taken as a reference standard.

2.8. Buffering capacity of DP nanoparticles

The buffering capacity of the series of DP₁₀ and DP₂₅ nanoparticles was determined over a pH range of 3–10 by an acid–base titration method, as described by Bennis et al.²⁵ Briefly, DP₁₀₋₁ nanoparticles (3 mg) were dissolved in an aqueous solution of sodium chloride (0.1 N, 30 ml). The pH of the solution was brought to 10 (by adding a solution of 0.1 N NaOH) and the resulting solution was titrated with a solution of 0.1 N HCl by pouring an aliquot of 25 μ l at a time until the pH of the solution reached 3. The pH of the solution was measured after each addition of HCl solution. Likewise, DP₁₀₋₂, DP₁₀₋₃, DP₁₀₋₄, DP₂₅₋₁, DP₂₅₋₂, DP₂₅₋₃, DP₂₅₋₄ and bPEI_{10,25} were dissolved in 0.1 N NaCl solutions and titrated. The pH titration curves for the series of DP₁₀ and DP₂₅ nanoparticles and native bPEI_{10,25} were drawn.

2.9. DNA release study

In order to assess the unpackaging of DNA from the complexes, DNA release assay was carried out. bPEI_{10,25}, DP₁₀ and DP₂₅ nanoparticles were complexed with pDNA (300ng/ μ l) at their best w/w ratios (where these complexes exhibited the highest transfection efficiency) and incubated for 30 min at an ambient temperature. Then heparin, a highly charged polyanion, was added increasing amounts which competed with pDNA and released the bound pDNA from the complexes. The samples were then incubated for 30 min, mixed with 2 μ l Orange G dye and electrophoresed (100 V, 1 h) in a 0.8% agarose gel containing EtBr and visualized on a UV transilluminator using Syngene Gel Doc System.

2.10. In vitro transfection studies

Capability of DP₁₀ and DP₂₅ nanoparticles to carry plasmid DNA inside the cells was assessed by in vitro transfection assay on MCF-7 cells. The cells were seeded in a 96-well plate at a density $\sim 6 \times 10^3$ cells/well in complete medium (DMEM containing 10% FBS) and incubated at 37°C for 24 h in a humidified environment in CO₂ incubator. Transfection was carried out at 70–75% confluency. The media was aspirated and cells washed once with 1x PBS (50 μ l in each well). bPEI₁₀/pDNA, bPEI₂₅/pDNA, DP₁₀/pDNA and DP₂₅/pDNA complexes were prepared at different w/w ratio of 0.66, 1.33, 2.33, 3.33, 4, 5, 6.66 and 10 in DMEM. For comparative analysis, Lipofectamine/pDNA complex was also prepared following manufacturer's protocol. These complexes were incubated for 30 min at an ambient temperature and then gently added on to the cells. The plate was kept in the incubator at 37°C in a humidified CO₂ incubator. After 3 h, the

transfection mixture was aspirated out and fresh complete media (DMEM containing 10% FBS; 100 μ l) was added to the cells in each well. Cells were further incubated at 37°C in CO₂ incubator for 45h. The cells were then visualized for GFP expression under inverted fluorescence microscope and captured the images.

2.11. Quantification of GFP expression

The quantity of the GFP gene expression in transfected cells was estimated on Nanodrop ND-3000 spectrofluorometer. After 48 h of transfection, the cells were washed with 1x PBS and further incubated with 50 μ l of cell lysis buffer for 45 min at 37°C. Then 2 μ l of cell lysates were placed on Nanodrop to estimate protein spectrofluorometrically. 1x PBS was used as a blank to calibrate the spectrofluorometer to zero reading. The ELISA plate reader was used to estimate total protein content at 590 nm using Bradford's reagent with bovine serum albumin (BSA) as the standard. GFP fluorescence was expressed as arbitrary units (A.U.) / mg of protein.

2.12. Cell viability assay

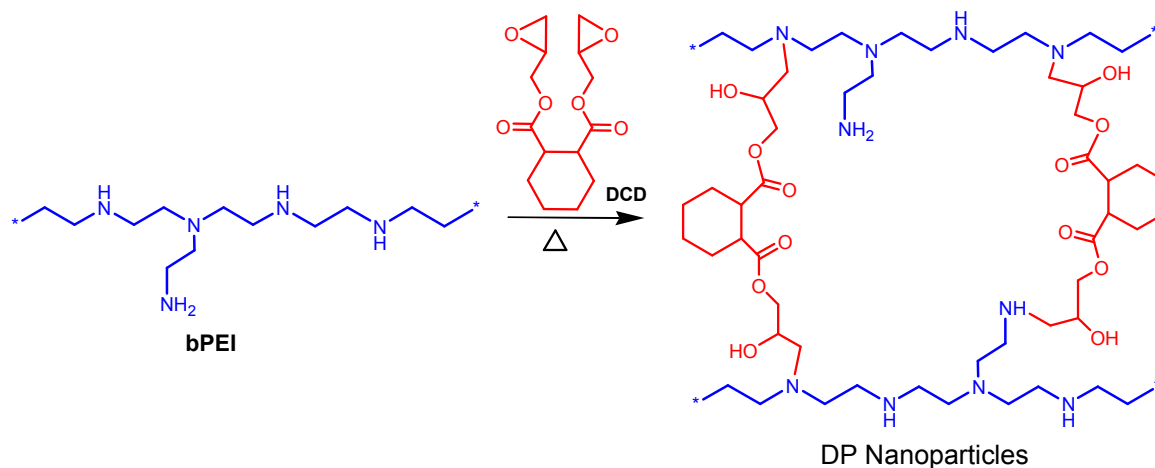
Cytotoxicity of DP₁₀/pDNA, DP₂₅/pDNA, bPEI₁₀/pDNA, bPEI₂₅/pDNA and Lipofectamine/pDNA complexes was evaluated on MCF-7 cells by MTT colorimetric assay. The assay involves the reduction of tetrazolium group (yellow color) by mitochondrial succinate dehydrogenase in live cells into formazan crystals (dark purple). After 48 h of transfection, media was aspirated and MTT reagent (100 μ l, 1mg/ml) dissolved in DMEM was added to the cells. The plate was kept in a humidified CO₂ incubator for 2 h at 37°C. After incubation, the supernatant was aspirated and the formazan crystals were dissolved in 100 μ l of isopropanol containing SDS (0.5%) and HCl (0.06M). Intensity of the color was measured spectrophotometrically on an ELISA plate reader (MRX, Dynatech Laboratories) at 570 nm and untreated cells were taken as control with 100% viability. Cells without addition of MTT were taken as blank to calibrate the spectrophotometer to zero absorbance. Experiment was repeated in triplicate and percent cell viability was calculated using the formula:

$$\text{Cell viability (\%)} = A_{\text{transfected}} / A_{\text{control}} \times 100$$

3. Results and discussion

The main objective of the present investigation was to develop an efficient delivery system devoid of cytotoxicity. The polymers were crosslinked to convert them into their respective nanoparticles for the following reasons, viz., (i) crosslinking would reduce the charge density on the nanoparticles, hence help in rendering these nanoparticles less toxic, (ii) small-sized nanoparticles would enter into the cells easily exhibiting higher uptake and internalization, and (iii) reduced charge density on nanoparticles would facilitate easy disassembly of the complexes inside the cells, thereby releasing pDNA for higher gene expression. These factors not only resulted in higher transfection efficiency but also improved the cell viability significantly.

Synthesis of DP nanoparticles was achieved in a single-step reaction between amine groups (primary and secondary) of branched PEI (10 and 25 kDa) and epoxy groups of the crosslinker, diglycidyl-1,2-cyclohexanedicarboxylate (DCD), as depicted in scheme 1. It is a well known reaction in the literature wherein the secondary amines, being stronger nucleophiles, react more readily than primary amines. However, here, in polyethylenimine, primary amines are available on the periphery (more exposed position) while secondary amines reside on the polymer backbone (slightly buried inside). Based on these structure features, it was assumed that during the reaction, primary amines would react more readily with DCD. In the schematic representation, crosslinking reaction among the amines has been shown randomly. It does not provide the exact ratio of primary and secondary amines involved in the reaction between bPEI and DCD. It depends upon the arrangement and orientation of the functionalities in the polymeric structure.



Scheme 1. Synthesis of crosslinked DP nanoparticles.

By varying the amount of DCD, two series of nanoparticles (DP₁₀ and DP₂₅) with crosslinking (2, 4, 6 and 8%) were prepared. Attempts to prepare nanoparticles with higher crosslinking (10% or more) could not be achieved as these nanoparticles showed poor dispersibility after lyophilization. Therefore, we kept the percent crosslinking upto 8% in both the cases. The introduction of the crosslinker into the synthesized nanoparticles was confirmed by ¹H-NMR spectroscopy (Fig. S1, *pl. see Supplementary Information*). Peaks at δ 2.4–3.4 ppm showed the presence of PEI protons (-NCH₂-, -NH-CH₂-, -CH₂NH₂) while protons at δ 1.1-1.2 and δ 3.9 ppm corresponded to methylene (-CH₂-) and -OCH- and -OCH₂- groups. This confirmed the chemical crosslinking of bPEI with DCD. Further, the percent substitution of the crosslinker in the nanoparticles was determined by FDNB assay (Fig. 1). Results (Table-1) revealed the substitution pattern as DP₁₀-1 (2%, 1.26%), DP₁₀-2 (4%, 2.72%), DP₁₀-3 (6%, 3.93%), DP₁₀-4 (8%, 4.79%), DP₂₅-1 (2%, 1.13%), DP₂₅-2 (4%, 2.25%), DP₂₅-3 (6%, 2.8%) and DP₂₅-4 (8%, 5.3%). First value in the parenthesis corresponds to attempted percentage and second value is the actual percent substitution. The percent crosslinking in the nanoparticles varied from ~47 – 68% of the attempted crosslinking.

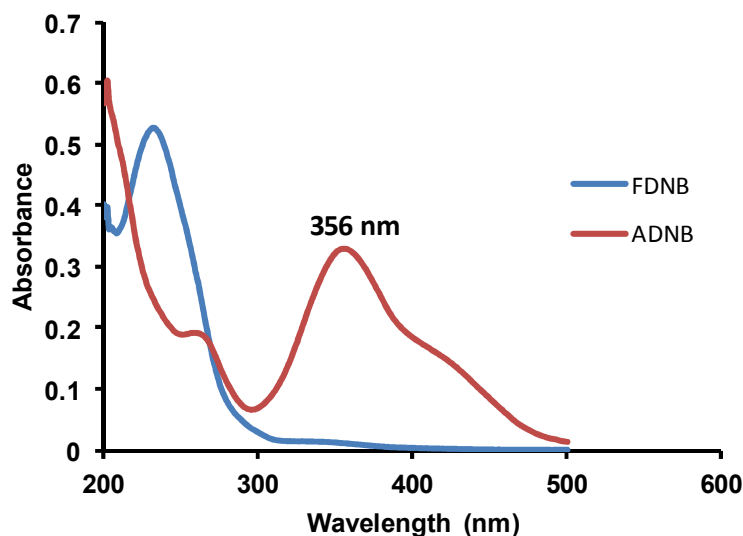


Figure 1. UV spectra of 1-fluoro-2,4-dinitrobenzene (FDNB) and polyethylenimine-treated FDNB (1-aminated-2,4-dinitrobenzene, ADNB).

Table-1. Determination of degree of substitution in the DP nanoparticles by 2,4-dinitrofluorobenzene (FDNB)

| Samples | Attempted substitution (%) | Found substitution (%) |
|---------------------|----------------------------|------------------------|
| DP ₁₀ -1 | 2 | 1.26 |
| DP ₁₀ -2 | 4 | 2.72 |
| DP ₁₀ -3 | 6 | 3.93 |
| DP ₁₀ -4 | 8 | 4.79 |
| DP ₂₅ -1 | 2 | 1.13 |
| DP ₂₅ -2 | 4 | 2.25 |
| DP ₂₅ -3 | 6 | 2.81 |
| DP ₂₅ -4 | 8 | 5.32 |

The hydrodynamic diameter of bPEIs (10 and 25 kDa), DP nanoparticles resulting from crosslinking of bPEIs and their pDNA complexes was determined by dynamic light scattering (DLS). Native bPEIs, without any defined structure, showed average size (hydrodynamic diameter) ~370-380 nm with high polydispersity. When these two polymers were crosslinked with varying amounts of DCD, the average particle size in both the series of DP₁₀ and DP₂₅ nanoparticles was found to be in the range of 153-218 nm and 134-261 nm, respectively (Table 2). As the amount of crosslinker increased, the average size of particles decreased suggesting more compactness in the structures. On interaction with negatively charged pDNA, there was a further decrease in the overall size of the particles. It changed to 125-150 nm and 162-207 nm in DP₁₀/pDNA and DP₂₅/pDNA complexes, respectively (Table-2). However, in case of pDNA complexes of DP₂₅-3 and DP₂₅-4, average size of the complexes increased, which could be attributed to swelling of the complexes to a greater extent. Similarly, in zeta potential measurements, pDNA complexes of native bPEI (10kDa) and bPEI (25 kDa) showed their surface charge ~+26 and 29 mV, which decreased drastically in case of nanoparticle formulations. This change in surface charge might be due to conversion of polymers into nanoparticles, which changed the ratio of primary, secondary and tertiary amines as

well as some of the charge might get buried inside the pore and hence, inaccessible for measurement/interaction. The zeta potential of both the series of complexes was found to be in the range of $\sim +15$ -19 mV (DP₁₀/pDNA complexes) and +11-20 mV (DP₂₅/pDNA complexes) as shown in table-2. Lowest zeta potential recorded in case of DP₁₀-3 and DP₂₅-2 nanoparticles might be attributed to orientation / spatial arrangement of polymeric chains in the nanoparticles so that higher amount of charge was not available for measurement.

Table-2. Average particle size (hydrodynamic diameter) and zeta potential measurements of DP₁₀ and DP₂₅ nanoparticles and their pDNA complexes

| Samples | Average particle size (d. nm) \pm S.D. | | Zeta potential mV \pm S.D. |
|---------------------|---|------------------------------------|------------------------------------|
| | Native | pDNA complex (H ₂ O) | pDNA complex (H ₂ O) |
| bPEI ₁₀ | 370.7 \pm 52.31 | 201.6 \pm 21.36 | 26.48 \pm 0.35 |
| DP ₁₀ -1 | 218.1 \pm 7.56 | 128.0 \pm 3.41 | 18.8 \pm 0.66 |
| DP ₁₀ -2 | 200.9 \pm 6.34 | 131.2 \pm 4.79 | 18.3 \pm 0.21 |
| DP ₁₀ -3 | 197.0 \pm 6.78 | 150.1 \pm 3.45 | 15.0 \pm 0.64 |
| DP ₁₀ -4 | 152.7 \pm 7.21 | 125.1 \pm 4.48 | 16.0 \pm 0.65 |
| bPEI ₂₅ | 380.2 \pm 54.8 | 244.0 \pm 23.89 | 29.48 \pm 0.57 |
| DP ₂₅ -1 | 260.5 \pm 5.37 | 201.0 \pm 4.27 | 12.0 \pm 1.10 |
| DP ₂₅ -2 | 186.5 \pm 4.32 | 162.3 \pm 6.24 | 11.4 \pm 1.00 |
| DP ₂₅ -3 | 154.9 \pm 4.11 | 207.3 \pm 5.65 | 14.5 \pm 0.40 |
| DP ₂₅ -4 | 134.4 \pm 3.58 | 183.5 \pm 8.98 | 20.0 \pm 1.86 |

Further, transmission electron microscopic (TEM) analysis revealed the formation of spherical shaped DP₁₀-2/pDNA and DP₂₅-4/pDNA complexes, typically of the order of ~ 30 –50 nm in size (Figure 2). The particle size was smaller than that observed by DLS. In DLS, the size of the particle is measured along with solvent molecules attached to the surface of these particles (i.e. true state of nanoparticles in medium). Moreover, DLS provides the intensity-based size distribution which also accounts for aggregated particles. While, in case of TEM, number-based size

distribution is obtained as it measures the particle size in a dry state. There are several reports available in the literature where a significant difference in the particle size distribution has been observed between DLS and TEM.²⁶ The projected results are in complete agreement with the previous findings.

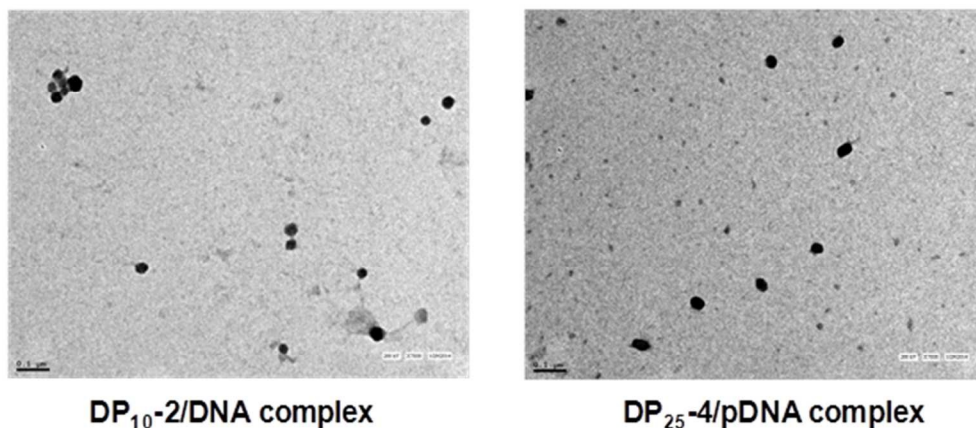
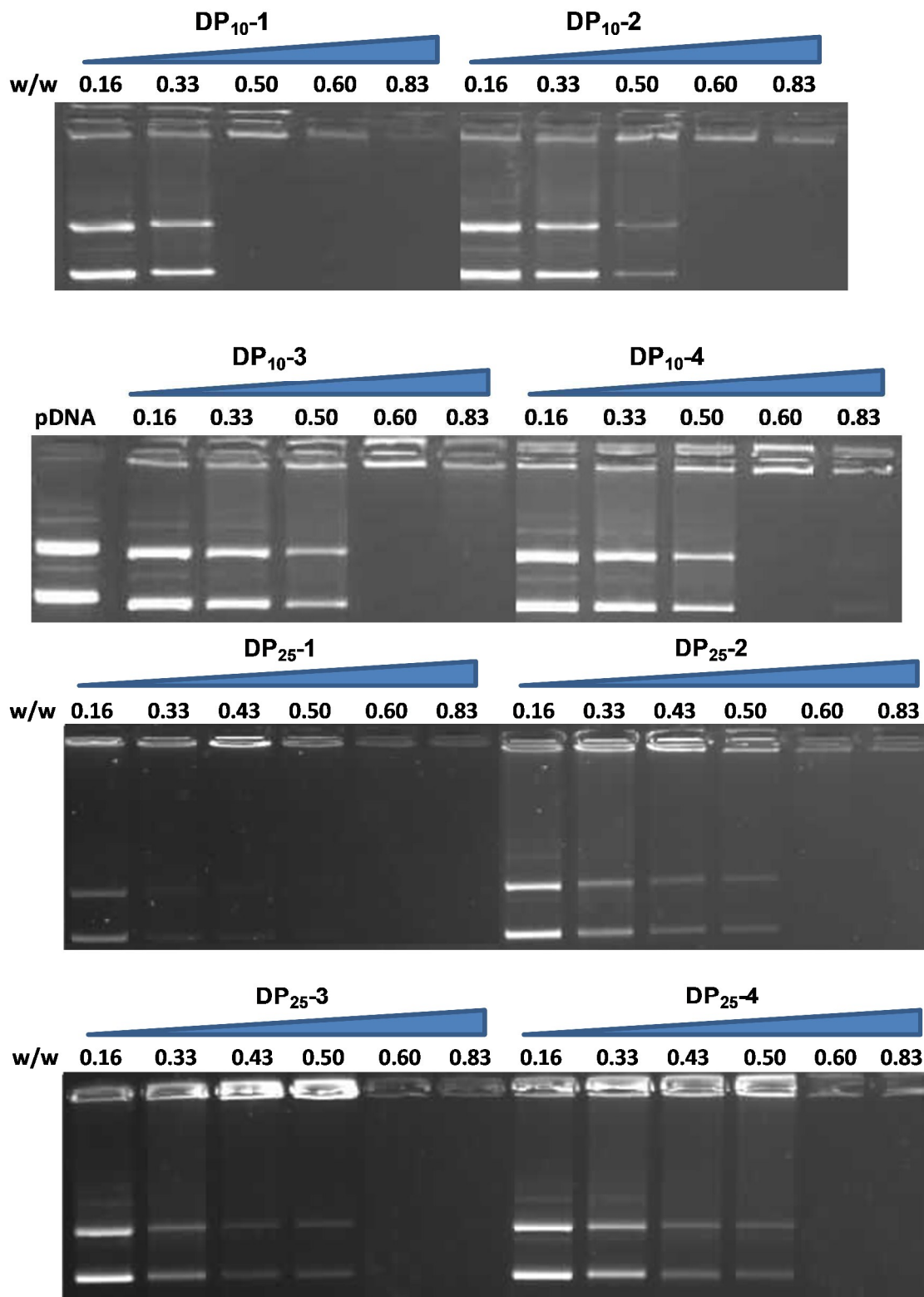


Figure 2. Transmission electron microscopic images of pDNA complexes of DP₁₀-2 and DP₂₅-4 complexes. Size of the complexes were in the range of 30-50 nm. Scale bars in both the images correspond to 0.1 μm .

Agarose gel electrophoresis (0.8% agarose gel) was performed to assess the DNA binding efficacy of DP nanoparticles. The optimal concentration required of the DP nanoparticles to bind pDNA (300ng/ μl) and retard its mobility on the agarose gel was analyzed by carrying out the assay at different w/w ratios. DP₁₀-1 and DP₂₅-1 nanoparticles, bPEI₁₀ and bPEI₂₅ retarded the mobility of pDNA at w/w ratio of 0.5, while other nanoparticles retarded the mobility of same amount of pDNA at w/w ratio of 0.6 (Fig. 3). This could be attributed to the fact that due to conversion of primary and secondary amines to secondary and tertiary amines, respectively, on the reaction of bPEIs with DCDAs well as formation of nanoparticles wherein a fraction of charge might get buried inside the nanoparticle core. The buried charge might not be accessible for binding negatively charged pDNA and this might cause a decrease in the overall charge on the nanoparticles. Therefore, DP nanoparticles with 4-8% crosslinking showed retardation at slightly higher w/w ratio, i.e. DP₁₀-2,3,4 and DP₂₅-2,3,4 were required in higher amounts to retard the movement of the fixed amount of pDNA.



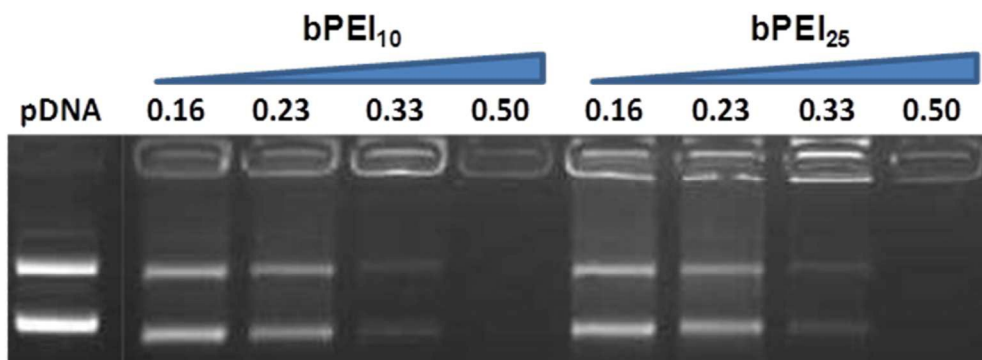


Figure 3. Mobility shift assay of pDNA complexes of both the series (DP₁₀ and DP₂₅), bPEI₁₀ and bPEI₂₅ at various w/w ratios.

There are various approaches which describe that early endosomal escape of complexes is beneficial and prevents internalization of these complexes in the lysosomal compartments. For cationic polymers, proton-sponge hypothesis has been proposed. However, for cationic polymers lacking buffering capacity, endosomolytic agents are needed to get their complexes released from the endosomes into the cytosol. Polyethylenimine is a unique polymer which contains three types of amines (1^o, 2^o, and 3^o) and high charge density which inhibit activity of endosomal nucleases and causes endosomal swelling followed by rupturing.²⁷⁻²⁹ Therefore, buffering capacity plays a crucial role in non-viral vector-mediated delivery of nucleic acids.

To determine the effect of crosslinking on the buffering capacity of the resulting nanoparticles, the standard acid-base titrations were carried out.²⁵ The results revealed that on conversion of native polymers into their respective nanoparticles, there was a significant change in the buffering capacity. In both the series, buffering capacity of the nanoparticles decreased (Fig. 4), however, it was still found to be enough for the complexes to escape from the endosomes. This was established from the transfection assay where DP nanoparticle/pDNA formulations exhibited higher transfection efficiency as compared to native bPEI complexes. There are also a number of reports cited in the literature, wherein a decrease in the buffering capacity of the vectors has been noticed and still, these systems have displayed much superior transfection efficiency.³⁰⁻³³

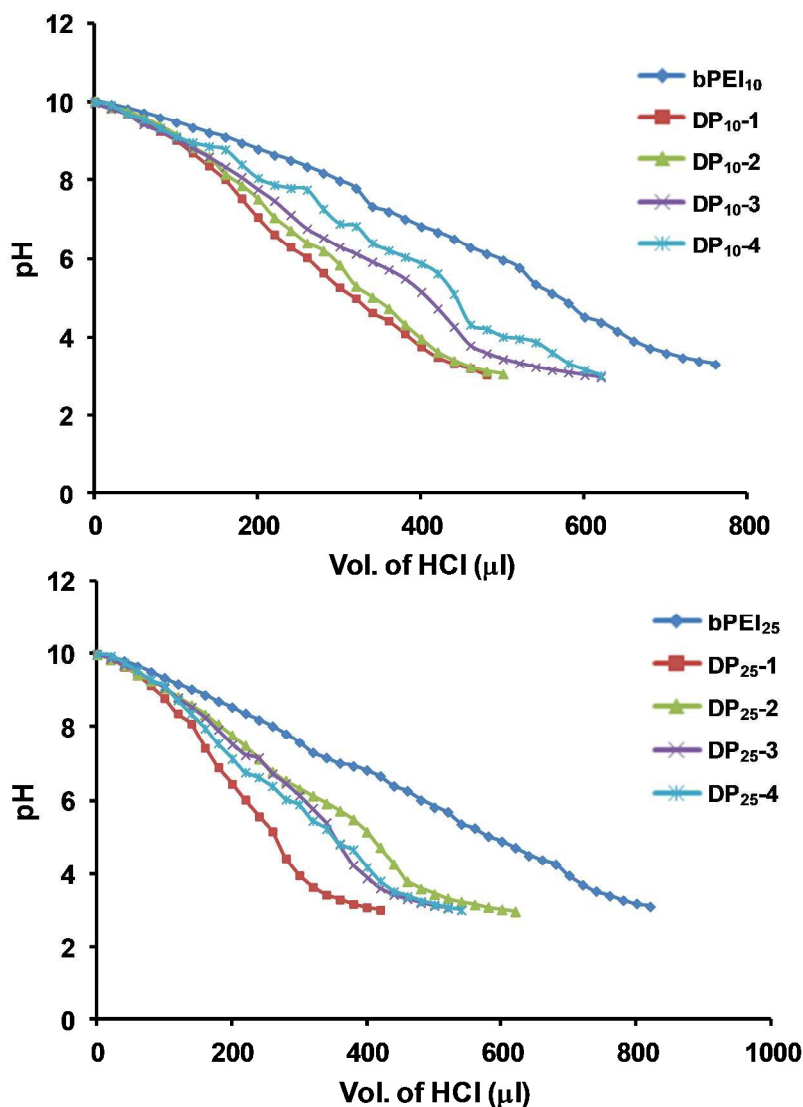


Figure 4. Acid-base titration profiles of DP₁₀ and DP₂₅ nanoparticles, and bPEI₁₀ and bPEI₂₅ polymers.

Further, to assess the impact of formation of nanoparticles on the stability of pDNA complexes, pDNA release from DP₁₀/pDNA and DP₂₅/pDNA complexes was monitored by the heparin release assay. The results were compared with the binding ability of native bPEI_{10,25}/pDNA complexes at their best working w/w ratios of 1.66 and 1.33, respectively using heparin in increasing amount in the reaction mixtures. Release of ~82-95% pDNA was observed from DP₁₀/pDNA complexes whereas only ~77% pDNA released from bPEI₁₀/pDNA complex as shown in figure 5. Similarly, the maximum release of ~81-96% pDNA was observed from DP₂₅/pDNA

complexes whereas ~61% pDNA was released from bPEI₂₅/pDNA complex (Fig. 5). The higher release in DP NPs might be attributed to partial decrease in cationic charge density (in particular 1° amine density) post-conversion of 1° and 2° amines to 2° and 3° amines, respectively, which resulted in the relatively loose binding of DP/pDNA complexes.

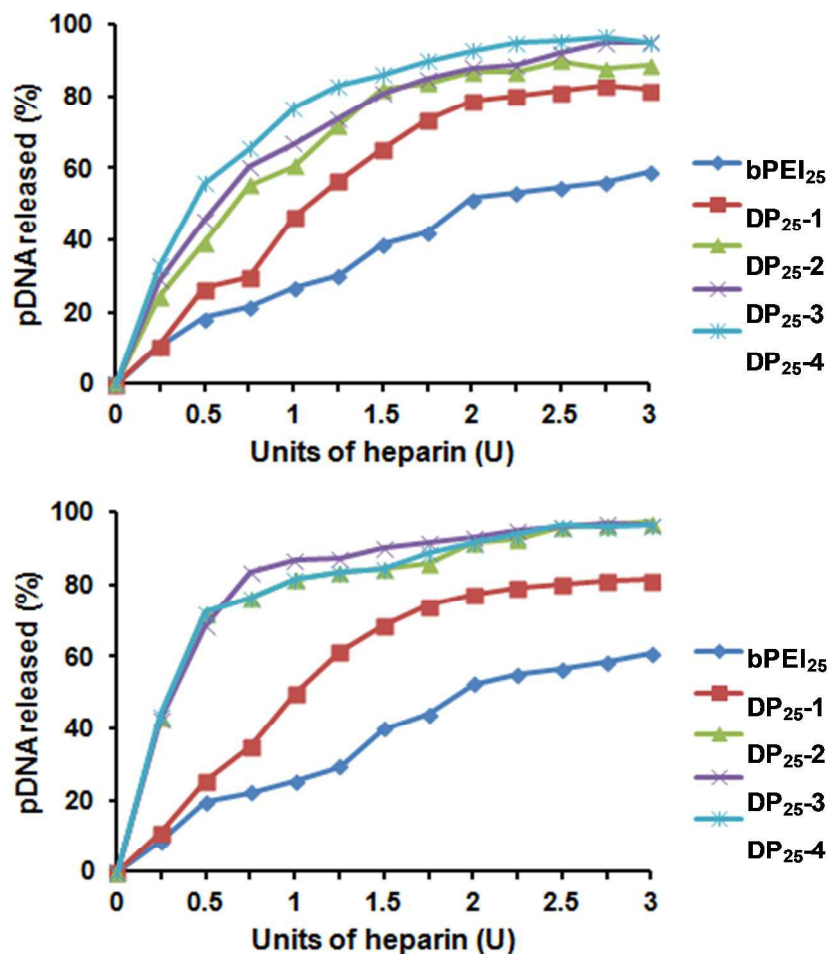


Figure 5. DNA release assay of pDNA complexes of DP₁₀ and DP₂₅ nanoparticles and bPEI₁₀ and bPEI₂₅ polymers using an anionic polymer, heparin, at their respective best working w/w ratios.

Further, to ensure the non-toxic behavior of pDNA complexes, cytotoxicity of DP/pDNA and bPEI_{10,25}/pDNA complexes was evaluated on MCF-7 cell line by MTT assay over a range of w/w ratios relevant to transfection assay. The cell viability of DP/pDNA complexes was found to be higher as compared to bPEI_{10,25}/pDNA complexes (Fig. 6), which might be due to the fact that after crosslinking, partially the primary amines (the main source of toxic charge)³⁴⁻³⁶ got converted into

secondary amines and secondary amines to tertiary amines (i.e. bad charge of primary amines converted into good charge of secondary and tertiary amines), thereby improving the cell viability. DP₁₀/pDNA and DP₂₅/pDNA complexes showed cell viability in the range of ~92-98% and 90-95%, respectively, while bPEI_{10,25}/pDNA complexes showed cell viability ~72% and 62%, respectively. These results show that these non-toxic vectors can be used effectively in gene delivery applications.

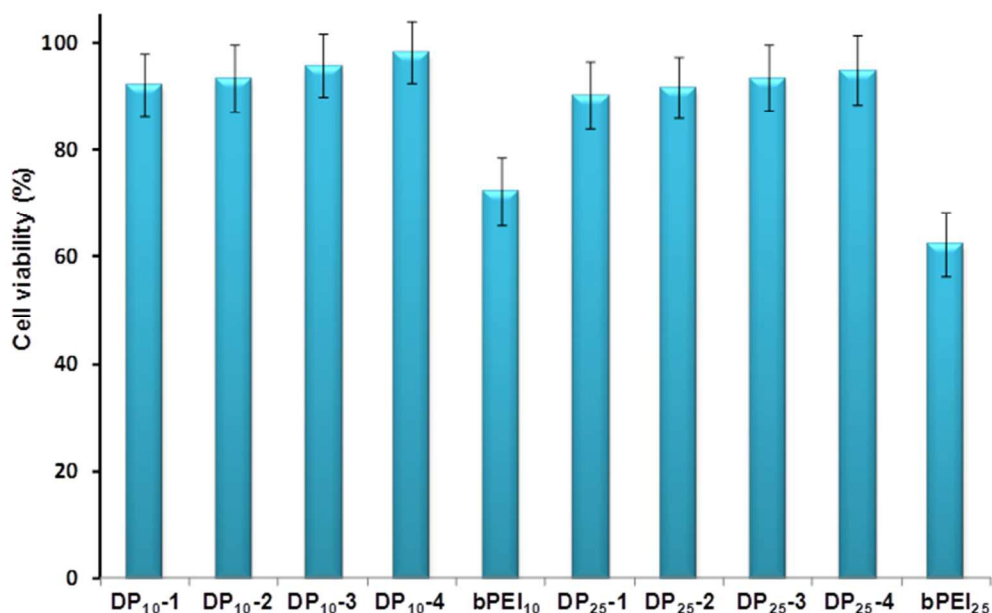


Figure 6. Cytotoxicity assay of pDNA complexes of DP₁₀ and DP₂₅ nanoparticles and bPEI₁₀ and bPEI₂₅ polymers prepared at their best working w/w ratios (overall charge +ve) using MTT reagent on MCF-7 cells. The experiment was performed in triplicate.

Having assessed for cytotoxicity and pDNA release, DP nanoparticles were evaluated for their capability to transport pDNA inside the MCF-7 cells for efficient gene expression. After 48h of transfection, cells were observed under inverted fluorescence microscope for GFP gene expression. Figure 7 depicts the expression pattern in the MCF-7 cells. After quantification, it was observed that DP/pDNA complexes exhibited higher transfection efficiency than their respective native bPEIs (Fig. 8). From the results, it was also observed that transfection efficiency varied with the w/w ratio. Initially, it increased upto a certain level and after achieving the highest transfection efficiency, it decreased. Among the two series of complexes, DP₂₅/pDNA complexes showed much higher transfection efficiency than DP₁₀/pDNA complexes. All the complexes of DP₁₀/pDNA

displayed higher transfection efficiency than native bPEI₁₀/pDNA complex with DP₁₀-2/pDNA complex exhibited the highest transfection

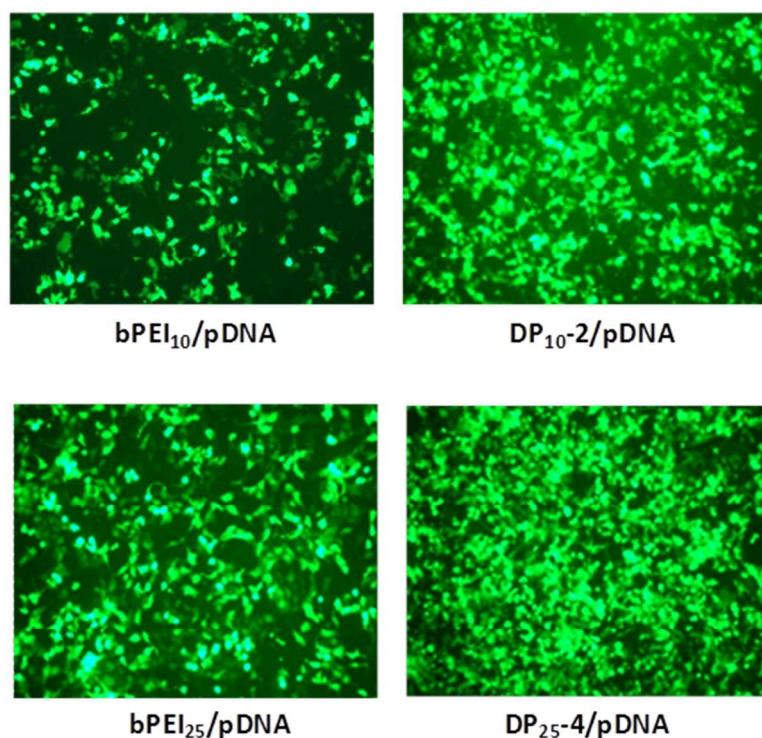


Figure 7. Fluorescence microscopic images of GFP gene transported by DP₁₀-2 and DP₂₅-4 nanoparticles and bPEI₁₀ and bPEI₂₅ polymers and expressed in MCF-7 cells at their best w/w ratios (overall +ve charge on the complexes).

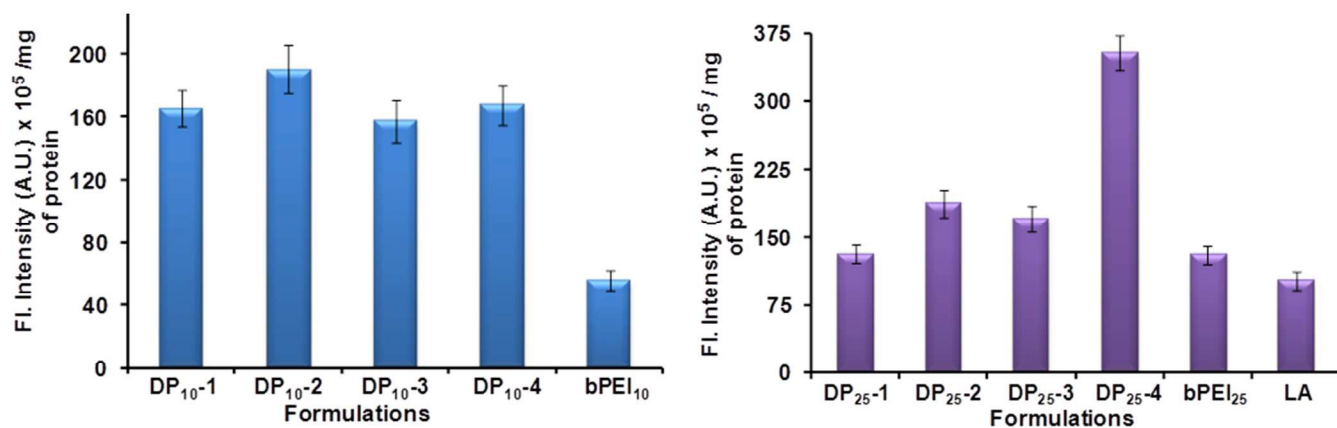


Figure 8. Gene transfection assay of DP₁₀/pDNA, DP₂₅/pDNA, bPEI₁₀/pDNA, bPEI₂₅/pDNA and Lipofectamine/pDNA complexes at their best w/w ratios (overall +ve charged) in MCF-7 cells. The experiment was carried out in triplicate.

efficiency i.e. ~ 3.4 folds higher than bPEI₁₀/pDNA complex. Similarly, DP₂₅/pDNA complexes showed higher transfection efficiency than bPEI₂₅/pDNA complex. These complexes even displayed higher transfection efficiency than the commercially available Lipofectamine/pDNA complex. Among various complexes, DP₂₅₋₄/pDNA complex exhibited the highest transfection efficiency, i.e. ~ 2.7 and 3.5 folds higher than bPEI₂₅ and Lipofectamine/pDNA complexes, respectively. DP₂₅₋₄/pDNA complex even showed ~ 1.9 folds higher transfection compared to DP₁₀₋₂/pDNA which showed its superiority. High transfection efficiency exhibited by these nanoparticles could be due to several factors such as surface charge, small size of the complexes, presence of hydrophobicity, molecular weight, easy unpackaging of the complexes inside the cells and low toxicity. Surface charge plays an important role in cell adhesion and endosomal escape of the complexes. Presence of cationic charge on the complexes makes them to interact with the negatively charged cell membranes and effects their internalization, which results in higher gene expression subsequent to endosomal escape. Small sized particles are efficiently taken up by the cells as compared to larger ones and move freely for nuclear localization. Apart from these factors, hydrophobicity and molecular weight further elevate the extent of binding with the lipophilic cell membrane followed by uptake of the complexes inside the cells. Additive effects of these factors along with easy disassembly of the complexes inside the cells result in the enhanced transfection efficiency. To arrive at the best possible formulation to display the highest transfection efficiency, a series of DP nanoparticles were synthesized and on evaluation, DP₂₅₋₄ was found to be best formulation which confirmed the optimal balance of all the parameters i.e. size, surface charge, degree of hydrophobicity, ease of disassembly, buffering capacity, etc. nsisted of appropriate degree of hydrophobicity-hydrophilicity, amount of charge, size and buffering capacity. Hence, it exhibited the highest transfection efficacy with low toxicity.

4. Conclusions

In summary, we have developed nanoparticle-based transfection reagents using branched polyethylenimine of two different molecular weights. By crosslinking these polymers separately and converting them into their respective nanoparticles, these were characterized physic-chemically and biologically. The crosslinker not only converted the branched polymers into their nanoparticles but also converted primary and secondary amines to secondary and tertiary amines, i.e. overall number of amines remained same. The projected protocol did not block the charge, which was the

highlighting feature of this strategy. Nanoparticles resulting from higher molecular weight polyethylenimine when complexed with pDNA showed several folds higher transfection efficiency than complexes of low molecular weight polymer, native polymers and Lipofectamine with almost non-toxic character implying that molecular weight does play an important role. These results show the potential of such vectors to mediate efficient gene delivery and can be used in future applications.

Acknowledgement

Authors gratefully acknowledge the financial support from the CSIR Network Project (BSC0112).

References

- 1 L. Zhu and R. I. Mahato, *Expert Opin. Drug Deliv.*, 2010, **7**, 1209-1226.
- 2 H. C. Kang, K. M. Huh and Y. H. Bae, *J. Control. Release* 2012, **164**, 256-264.
- 3 P. Midoux, C. Pichon, J. J. Yaouanc and P. A. Jaffrès, *Br. J. Pharmacol.*, 2009, **157**, 166-178.
- 4 D. Luo and W. M. Saltzman, *Nat. Biotechnol.* 2000, **18**, 33-37.
- 5 W. T. Godbey, K. K. Wu and A. G. Mikos, *J. Control. Release*, 1999, **60**, 149-60.
- 6 S. Di Gioia and M. Conese, *Drug Des. Dev. Ther.*, 2008, **2**, 163-188.
- 7 U. Lungwitz, M. Breunig, T. Blunk and A. Gopferich, *Eur. J. Pharm. Biopharm.*, 2005, **60**, 247-266.
- 8 S. Taranejoo, J. Liu, P. Verma and K. Hourigan, *J. Appl. Polym. Sci.*, 2015, **132**, 42096, doi: 10.1002/app.42096
- 9 W. T. Godbey, K. K. Wu and A. G. Mikos, *J. Biomed. Mater. Res.*, 1999, **45**, 268-275.
- 10 L. Jin, X. Zeng, M. Liu, Y. Deng and N. He, *Theranostics*, 2014, **4**, 240-255.
- 11 Y. Li, H. Tian, J. Ding, X. Dong, J. Chena and X. Chen, *Polym. Chem.*, 2014, **5**, 3598-3607.
- 12 D. Pezzoli, F. Olimpieri, C. Malloggi, S. Bertini, A. Volonterio and G. Candiani, *PLoS One* 2012, **7**, e34711.
- 13 M. A. Mintzer and E. F. Simanek, *Chem. Rev.*, 2009, **109**, 259-302.
- 14 R. Kircheis, L. Wightman and E. Wagner, *Adv. Drug Deliv. Rev.*, 2001, **53**, 341-358.

- 15 A. Kichler, *J. Gene Med.*, 2004, **6**, S3-S10.
- 16 W. Dong, S. Li, G. Jin, Q. Sun, D. Ma and Z. Hua, *Int. J. Mol. Sci.* 2007, **8**, 81–102.
- 17 Z. Liu, Z. Zhang, A. Zhou and Y. Jiao, *Prog. Polym. Sci.*, 2010, **35**, 1144–1162.
- 18 S. Kim, J. S. Choi, H. S. Jang, H. Suh and J. Park, *Bull. Kor. Chem. Soc.*, 2001, **22** 1069-1075.
- 19 Y. S. Siu, L. Li, M. F. Leung, K. L. D. Lee and P. Li, *Biointerphases*, 2012, **7**:16.
- 20 C. S. Cho, *ISRN Mater. Sci.*, 2012, **2012**, Article ID 798247.
- 21 C. Kim, Y. Lee, S. H. Lee, J. S. Kim, J. H. Jeong and T. G. Park, *Macromol. Res.*, 2011, **19**, 166-171.
- 22 L. Shang, K. Nienhaus and G. U. Nienhaus, *J. Nanobiotechnol.*, 2014, **12**:5.
- 23 M. Shi, J. Lu and M. S. Shoichet, *J. Mater. Chem.*, 2009, **19**, 5485-5498.
- 24 T. N. Al-Sabha and I. A. Hamody, *Arab. J. Chem.*, 2015, **8**, 465-473.
- 25 J. M. Benns, J. S. Choi, R. I. Mahato, J. S. Park and S. W. Kim, *Bioconjug. Chem.*, 2000, **11**, 637-645.
- 26 a) R. Goyal, R. Bansal, R. P. Gandhi and K. C. Gupta, *J. Biomed. Nanotechnol.*, 2014, **10**, 3269-3279; b) R. Goyal, S. K. Tripathi, S. Tyagi, A. Sharma, K. R. Ram, D. K. Chowdhury, Y. Shukla and K. C. Gupta, *Nanomedicine*, 2012, **8**, 167-175; c) R. Goyal, S. K. Tripathi, E. Vazquez, P. Kumar and K. C. Gupta, *Biomacromolecules*, 2012, **13**, 73-83
- 27 B. Singh, S. Maharjan, T. E. Park, T. Jiang, S. K. Kang, Y. J. Choi and C. S. Cho, *Macromol. Biosci.*, 2015, **15**, 622-635.
- 28 S. Tseng, S. Tang, M. Shau, Y. Zeng, J. Cherng and M. Shih, *Bioconjug. Chem.*, 2005, **16**, 1375-1381.
- 29 W. C. Tseng, T. Y. Fang, L. Y. Su and C. H. Tang, *Mol. Pharm.*, 2005, **2**, 224-232.
- 30 M. Mahato, G. Rana, P. Kumar and A. K. Sharma, *J. Polym. Sci. Polym. Chem.*, 2012, **50**, 2344-2355.
- 31 A. M. Funhoff, C. F. van Nostrum, G. A. Koning, N. M. E. Schuurmans-Nieuwenbroek, D. J. A. Crommelin and W. E. Hennink, *Biomacromolecules*, 2004, **5**, 32-39.
- 32 K. Miyata, M. Oba, M. Nakanishi, S. Fukushima, Y. Yamasaki, H. Koyama, N. Nishiyama and K. Kataoka, *J. Am. Chem. Soc.*, 2008, **130**, 16287-16294.

- 33 H. Uchida, K. Miyata, M. Oball, T. Ishii, T. Suma, K. Itaka, N. Nishiyama and K. Kataoka, *J. Am. Chem. Soc.*, 2011, **133**, 15524-15532.
- 34 E. Fröhlich, *Int. J. Nanomed.*, 2012, **7**, 5377-5391.
- 35 A. Zintchenko, A. Philipp, A. Dehshahri and E. Wagner, *Bioconjug. Chem.*, 2008, **19**, 1448-1455.
- 36 S. K. Tripathi, N. Gupta, M. Mahato, K. C. Gupta and P. Kumar, *Coll. Surf. B:Biointerface* 2014, **115**, 79-85.

GRAPHICAL ABSTRACT

Crosslinked PEI nanoparticles were synthesized, which efficiently transported DNA inside the cells with minimal cytotoxicity.

